Mantle flow, dynamic topography, and rift-flank uplift of Arabia

Amy Daradich*
Jerry X. Mitrovica } Department of Physics, University of Toronto, Toronto, Ontario M5S 1A7, Canada
Russell N. Pysklywec Department of Geology, University of Toronto, Toronto, Ontario M5S 3B1, Canada
Sean D. Willett Department of Earth and Space Sciences, University of Washington, Seattle, Washington 98195, USA
Alessandro M. Forte Department of Earth Sciences, University of Western Ontario, London, Ontario N6A 5B7, Canada

ABSTRACT

Rift-flank uplift adjacent to the Red Sea is asymmetric, i.e., a broad tilt of the entire Arabian plate along an axis parallel to the rift and more localized uplift on the African shoulder. A suite of models has been proposed to explain this pattern, but no model has considered the dynamic effects of large-scale mantle flow. Recent high-resolution images from seismic tomography show a massive, anomalously slow shear velocity structure that emerges from the core-mantle boundary beneath South Africa and that reaches close to the surface at the Red Sea. This buoyant megaplume has been identified as the driving mechanism for anomalously high topography in southern Africa and rifting in East Africa; in this paper we investigate its role in present-day African-Arabian topography. In particular, we present predictions of dynamic topography based on viscous-flow simulations initiated using seismically inferred mantle heterogeneity. These predictions demonstrate that viscous stresses associated with mantle flow are responsible for the long-wavelength signal in African-Arabian flank uplift. Our results do not preclude localized topographic contributions from other processes, particularly within the near field of the Red Sea.

Keywords: Arabia, rift-flank uplift, mantle flow, dynamic topography.

INTRODUCTION

Rifting of the Red Sea margin is thought to have begun in the early Oligocene. Uplift of the adjacent Arabian plate began in the early Miocene, although the most active uplift has occurred since the middle Miocene (i.e., after ca. 15 Ma) (Almond, 1986; Bohannon, 1989). Present-day topography across the Red Sea is asymmetric; with the exception of the Afar-Arabian dome, the topographic high on the African side of the Red Sea is more localized and subdued relative to its Arabian conjugate (Fig. 1A). In contrast, much of southwest Arabia reaches elevations of >1000 m, and high topography extends well into the plate interior. There is a distinct regional tilt of the entire Arabian plate from the Red Sea to the Persian Gulf, a distance >1000 km. This pattern of topography is commonly cited as a classic example of rift-flank uplift (e.g., Wernicke, 1985).

Many thermal and mechanical models have been developed to explain rift-flank uplift, and these have been applied with varying success to the Arabian margin (van der Beek et al., 1994). The models are distinguished by the dominance of thermal, mechanical, geometric, and melt processes. In thermal models, uplift can result from depth-dependent stretching (Royden and Keen, 1980) or from the heating of flanks by small-scale convection (Keen, 1985; Buck, 1986). Mechanical modeling indicates that upward flexure may occur if the lithosphere maintains finite strength during rifting (Braun and Beaumont, 1989; Weissel and Karner, 1989). Geometric models first presented by Wernicke (1985) explain the asymmetry of uplift in terms of a single low-angle detachment penetrating the entire lithosphere. Finally, extensive flank uplift may also result from magmatic underplating due to asthenospheric partial melting (Cox, 1980; White and McKenzie, 1989).

These disparate models generally assume a passive origin for rift formation, and they are largely concerned with flank uplift within a few hundred kilometers of the rift basin. Therefore, none of these mechanisms provides a good explanation for the broad tilting of the Arabian plate that extends from the flank of the Red Sea to the Persian Gulf at the foothills of the Zagros Mountains (Fig. 1A).

The tilt appears to be a young feature. Although the western Arabian Shield may have been above sea level for much of the Phanerozoic, it has undergone only a few kilometers of erosion (Bohannon, 1989) and thus is not likely to have been elevated until recently. Furthermore, late Mesozoic and Paleogene marine sedimentary deposits are preserved near the Red Sea coast in northern and southern Arabia, indicating post-Eocene surface uplift (Beydoun, 1991).

The geologic record provides additional clues to the origin of the tilting. Although passive rifting is thought to have produced the northwest-southeast–trending tholeiitic to transitional lavas seen in western Arabia, active mantle upwelling may have placed younger transitional to strongly alkalic lavas along north-south trends in Arabia (Almond, 1986; Camp and Roobol, 1992). These younger lavas are largely contemporaneous with the period of major crustal uplift (12 Ma to the present), and their alkalinity suggests a deep-mantle origin (Almond, 1986; Camp and Roobol, 1992).

The geologically inferred connection between deep-mantle processes and the development of topography provides a possible mechanism for the long-wavelength tilting of the Arabian plate. In this paper we argue that the tilting represents the dynamic response of the Arabian plate to viscous stresses associated with active, large-scale mantle flow. To support this argument, we present predictions of dynamic topography based on viscous-flow simulations constrained by seismically inferred mantle heterogeneity.

MANTLE-FLOW SCENARIO FOR THE TILTING OF ARABIA

Global tomographic analyses of seismic data sets have progressively improved the resolution of models of mantle structure below the African-Arabian region (e.g., Grand et al., 1997; Ritsema et al., 1999). Figure 2 shows three-dimensional images of two recent seismic models (Ritsema et al., 1999; Grand, 2002), where the red contour represents a specific shear-wave velocity perturbation (see caption) relative to a radial reference model. The plots highlight a large, seismically slow region at the base of the mantle under southern Africa that has previously been interpreted as an upwelling megaplume on the basis of high topography (Hager, 1984; Lithgow-Bertelloni and Silver, 1998) and geologically inferred uplift rate (Gurnis et al., 2000). The megaplume appears to connect at shallower depths with a structure that is thought to act as the driving mechanism for rifting in East Africa (Ritsema et al., 1999; Ritsema and van Heijst, 2000; Lithgow-Bertelloni and Silver, 1998). This shallow heterogeneity reaches the lithosphere southeast of the Red Sea, near the Afar triple junction, and ultimately spreads beneath the Red Sea–Arabian region.

Because mantle flow associated with the megaplume has been identified as the driving force for epeirogenic and tectonic deformation in Africa, it is logical to consider the implications of the structure, and in particular its shallowest parts, for the already-described tilt-

*E-mail: adaradich@physics.utoronto.ca.

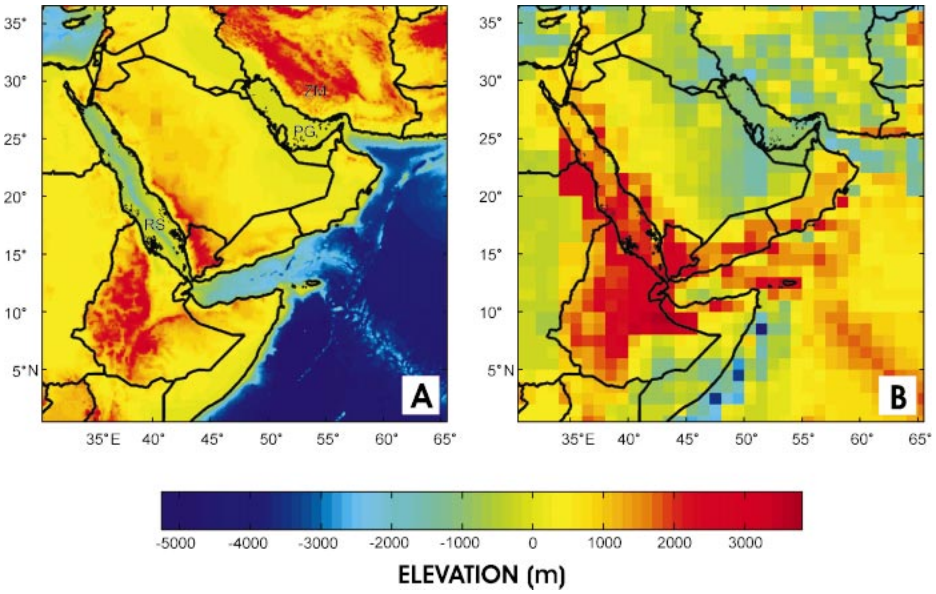

Figure 1. A: Topography of East African–Arabian region from ETOPO5 data set (http://www.ngdc.noaa.gov/mgg/global/seltopo.html). RS, PG, ZM—locations of Red Sea, Persian Gulf, and Zagros Mountains, respectively. B: Residual topography derived by correcting raw topography in frame A for crustal isostatic effects using crustal thickness and density model CRUST 2.0 (Laske et al., 2002).

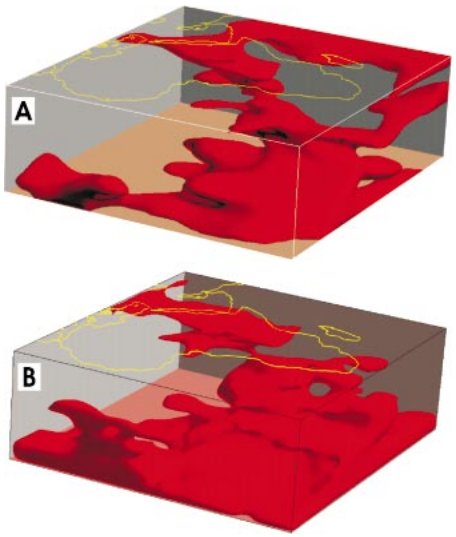

Figure 2. A: Three-dimensional image of −0.7% contour of mantle shear-wave velocity anomaly, based on S-wave velocity model S20RTS of Ritsema et al. (1999) within part of mantle underlying African-Arabian region. B: As in A, except for −0.6% contour of mantle shear-wave anomaly from seismic velocity model TXBW of Grand (2002). Cartesian projection extends from core-mantle boundary at bottom to Earth's surface at top. Model of Ritsema et al. (1999) is based on analysis of body-wave traveltimes, surface-wave phase velocities, and normal-mode splitting data. Grand (2002) analysis uses body-wave data, and is most recent in sequence of such models (e.g., Grand et al., 1997).

ing of the Arabian plate. Intuitively, viscous stresses associated with the material upwelling beneath the Red Sea flank of the Arabian plate would be expected to dynamically support uplift within this region. In the next section we quantify this scenario by using predictions of dynamic topography generated from mantle-flow simulations.

To isolate dynamic effects, our predictions will be compared to residual topography, i.e., the observed topography (Fig. 1A) corrected for crustal-thickness variations assuming isostatic compensation of the crust. We have adopted the model CRUST 2.0 (Laske et al., 2002) for this purpose. CRUST 2.0 provides both thickness and density of structures through the crust within $2° \times 2°$ cells. While this model is reasonably well constrained within the Arabian region (Laske et al., 2002), uncertainties in the density structure of the lower crust may introduce errors in the topographic correction. The residual topography (Fig. 1B) features a more pronounced tilt of the Arabian platform—including a dynamic depression of ~1000 m in the vicinity of the Persian Gulf—and higher peak topographies on both shoulders of the Red Sea.

FORMULATION OF NUMERICAL MODEL AND RESULTS

Our mantle-flow calculations are based on a spherical, two-dimensional (axially symmetric) finite-difference formulation of the equations that govern the conservation of mass, energy, and momentum of an incompressible Newtonian fluid having an infinite Prandtl number (Solheim and Peltier, 1994). The model involves the entire mantle, from the core-mantle boundary to the surface, and spans an angular distance of 140° (Fig. 3). Our use of a two-dimensional model is motivated by computational limitations, but it is justified, to first order, by the observed symmetry of the Arabian tilt (Fig. 1). That is, with the exception of the African-Arabian dome, the residual topography of the region is dominated by variations perpendicular to the trend of the Red Sea.

We first prescribe a density, or buoyancy, field within the model domain by using results from seismic tomography (see subsequent discussion). Second, the governing equations are solved for instantaneous flow fields throughout the domain. Third, dynamic topography is computed by applying surface-normal stresses output from the convection code to a model of elastic-beam deformation. We assume that the beam has a uniform flexural rigidity, with the exception of a break associated with the plate boundary in the Red Sea. Estimated values for the flexural rigidity of the Arabian lithosphere in the Red Sea region range from 3×10^{22} to 2×10^{24} N·m (van der Beek et al., 1994). We found that the predicted long-wavelength topographic variation is relatively insensitive to the choice of rigidity within this range.

The mantle-buoyancy field is prescribed by converting seismic velocity anomalies from the tomography models of both Grand (2002) and Ritsema et al. (1999) (Fig. 2) into density anomalies. This conversion is performed by using the depth-dependent velocity-to-density scaling profile of Forte and Woodward (1997). This scaling was modified from an earlier profile of Karato (1993) using constraints from a variety of geodynamic observations. The conversion assumes that the shear-wave velocity anomalies originate from temperature variations, although we note that recent work suggests that the African megaplume structure may also partially reflect variations in iron content (Forte and Mitrovica, 2001; Ni et al., 2002).

Figure 3 shows a density heterogeneity field prescribed in this manner superimposed on our numerical model domain. In the deep mantle, southwest of Arabia, the cross section is dominated by the buoyant (hot) megaplume structure already described. As in Figure 2, this feature appears to connect with shallower, buoyant material that impinges under the Red Sea side of the Arabian plate. The northeastern side of the Arabian plate is underlain by dense (colder than average) material extending through the entire upper mantle.

One final issue in the modeling involves heterogeneity in the shallowest (top 200 km) of the mantle. Because we assume a thermal origin for seismic velocity anomalies, negative buoyancy would be ascribed to regions where chemical heterogeneities contribute to seismically fast velocity anomalies in the shallow mantle below continents, i.e., in the neutrally

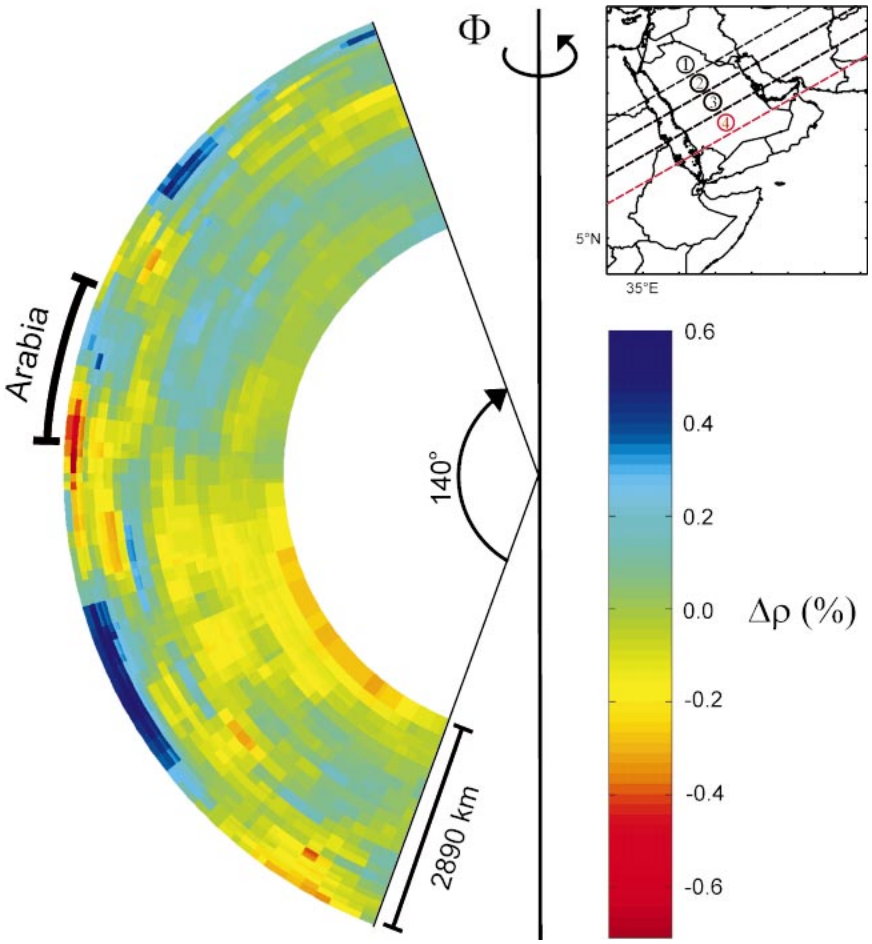

Figure 3. Geometry of axially symmetric solution space used in our viscous-flow simulations. Model domain extends 2890 km from core-mantle boundary to surface and across 140° arc relative to pole of axial symmetry (denoted by Φ). Free-slip conditions are applied across all boundaries of solution space, and numerical grid is defined by 257 nodes in radial direction and 769 nodes in direction of increasing azimuth. Within this model domain, we superimpose density heterogeneity in vertical cross section, with orientation given by profile 4 (highlighted in red in inset). Density field is obtained by scaling S-wave velocity model of Grand (2002) using velocity-to-density conversion profile described in text. Inset: Orientation of four vertical cross sections through seismic S-wave models used to initiate our two-dimensional numerical simulations.

buoyant ''tectosphere'' (Jordan, 1978). To overcome this difficulty, we zero out seismically fast heterogeneity in the top 200 km of the mantle. However, we note that simulations with and without this procedure applied showed only minor differences (on the order of 100 m) in the computed dynamic topography.

Our two-dimensional simulations were initiated with the heterogeneities taken from the four vertical cross sections specified in the inset of Figure 3. The average dynamic topography predicted from these four numerical runs, using heterogeneity based on the Grand (2002) seismic model, is shown in Figure 4 (dotted line), which is then compared to the range of residual topography computed from Figure 1B across the same four profiles (shaded region, Fig. 4). The predicted dynamic topography provides a close fit to the flank uplift and broad tilt of the Arabian platform. Specifically, viscous flow associated with large-scale mantle-density structure supports a total differential deflection of ~2.2 km from the topographic high at the flank of the Red Sea Margin to a low at the Persian Gulf.

The remaining dynamic topography curves in Figure 4 explore the sensitivity of our results to various aspects of the modeling. The dashed curve in Figure 4 is analogous to the dotted curve with the exception that the former is derived by adopting the seismic model of Ritsema et al. (1999) for mantle heterogeneity (Fig. 2A). The fit to the Arabian residual topography (shaded region) is comparable for this model choice. For the dashed-dotted result, we return to the Grand (2002) model, but we delete all mantle heterogeneity below 670 km depth. The close agreement between the dotted and dashed-dotted curves indicates that upper-mantle structure is largely responsible for the flow-induced tilting of the Arabian plate.

Our calculations do not predict the large peak in African residual topography within a few hundred kilometers of the Red Sea. This misfit may be due to various shortcomings of our model, including the resolution of the seismic model, the simplicity of the lithospheric structure adopted in the elastic-beam calculation, or the two-dimensional modeling approach. We note also that the raw topography shows significantly less uplift than the residual topography on the African shoulder of the Red Sea (cf. Figs. 1A and 1B), and thus the misfit in Figure 4 depends on the accuracy of the crustal model at this location.

Our modeling does not preclude that one of the many rift-flank processes described in the introduction may contribute to short-wavelength topography on either side of the Red Sea rift. Similarly, the topographic low observed in the Persian Gulf is, in part, due to topographical loading by the thickened crust in the Zagros-Taurus collision zone. Although we have accounted for that part of the thickened crust that is locally compensated, there is a flexural depression of the Arabian plate that we have not accounted for. This depression is likely to contribute to the topographic low in the Persian Gulf, but not in the Arabian plate interior.

CONCLUSIONS

We conclude that topography dynamically supported by large-scale viscous flow in the mantle is responsible for the dramatic tilting of the Arabian platform. The high topography of the Arabian rift flank is largely driven by upper mantle structure, which appears to be connected to the seismically slow and thermally buoyant megaplume structure (Fig. 2) that has previously been associated with the anomalous uplift of southern Africa and rifting in East Africa. The tilting is also enhanced by seismically fast (cold, dense) mantle beneath northeast Arabia (>200 km depth), which acts to dynamically depress the overlying plate in this area. Our results do not preclude shorter wavelength topographic effects on the margin of the Red Sea associated with one or more of the proposed mechanisms for flanking uplift at passive rifts (discussed in the introduction). We also acknowledge the contribution of loading of the Zagros Mountains to flexure of the Arabian plate in the vicinity of the Persian Gulf.

Connections among mantle heterogeneity, viscous flow, and the recent dynamics of the Arabian platform may also be explored by using regional gravity-field observations and, in particular, inferences of seismic anisotropy. Recent studies have revealed a coherent pattern of anisotropy beneath the Arabian shield

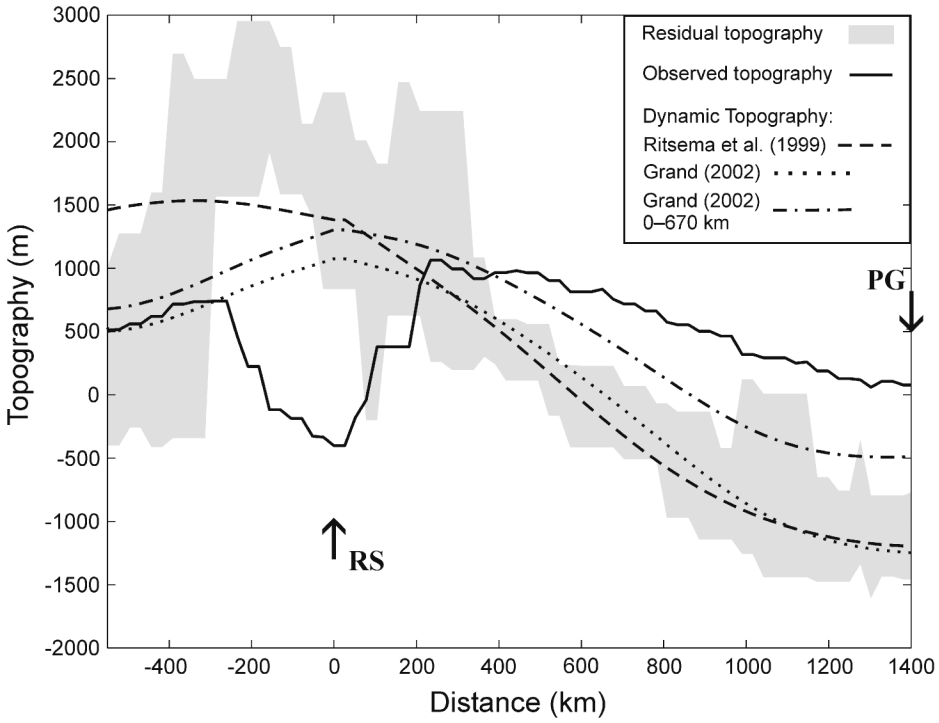

Figure 4. Minimum and maximum values of residual topography (shaded region) from Figure 1B computed across four profiles shown in inset of Figure 3. Observed (i.e., raw) topography (solid curve) is averaged across same four profiles. Dynamic topography (dashed curve and dotted curve) is computed by averaging results from two-dimensional numerical predictions across same four profiles; these viscous-flow predictions were initiated by using vertical cross sections of S-wave heterogeneity adopted from Grand (2002) or Ritsema et al. (1999) and scaled to density by using conversion profile discussed in text. Dashed-dotted curve is analogous to dotted; however, in this case we have deleted all mantle heterogeneity below 670 km depth (i.e., in lower mantle). RS and PG—locations of Red Sea and Persian Gulf, respectively.

(Wolfe et al., 1999; Levin and Park, 2000). Investigating the role of viscous flow on this signal requires three-dimensional simulations of mantle convection; future work should extend the present analysis for this purpose.

ACKNOWLEDGMENTS

We acknowledge support from the Natural Sciences and Engineering Research Council and the Canadian Institute for Advanced Research. We thank the reviewers for their constructive comments, as well as Miaki Ishii, Chris Guzofski, and Phillipe Fullsack for their various important contributions to this work.

REFERENCES CITED

Almond, D.C., 1986, Geological evolution of the Afro-Arabian dome: Tectonophysics, v. 131, p. 301–322.

Beydoun, Z.R., 1991, Arabian plate hydrocarbon geology and potential: A plate tectonic approach: American Association of Petroleum Geologists Studies in Geology, v. 33, 77 p.

Bohannon, R.G., 1989, The timing of uplift, volcanism and rifting peripheral to the Red Sea: A case for passive rifting?: Journal of Geophysical Research, v. 94, p. 1683–1701.

Braun, J., and Beaumont, C., 1989, A physical explanation of the relation between flank uplifts and the breakup unconformity at rifted continental margins: Geology, v. 17, p. 760–764.

Buck, W.R., 1986, Small-scale convection induced by passive rifting: The cause for uplift of rift shoulders: Earth and Planetary Science Letters, v. 77, p. 362–372.

Camp, V.E., and Roobol, M.J., 1992, Upwelling asthenosphere beneath western Arabia and its regional implications: Journal of Geophysical Research, v. 97, p. 15,255–15,271.

Cox, K.G., 1980, A model for flood basalt vulcanism: Journal of Petrology, v. 21, p. 629–650.

Forte, A.M., and Mitrovica, J.X., 2001, Deep-mantle high-viscosity flow and thermochemical structure inferred from seismic and geodynamic data: Nature, v. 410, p. 1049–1056.

Forte, A.M., and Woodward, R.L., 1997, Seismic-geodynamic constraints on three-dimensional structure, vertical flow, and heat transfer in the mantle: Journal of Geophysical Research, v. 102, no. B8, p. 17,981–17,994.

Grand, S.P., 2002, Mantle shear-wave tomography and the fate of subducted slabs: Royal Society of London, Philosophical Transactions, Mathematical, Physical & Engineering Sciences, v. 360, no. 1800, p. 2475–2491.

Grand, S.P., van der Hilst, R.D., and Widiyantoro, S., 1997, Global seismic topography: A snapshot of convection in the Earth: GSA Today, v. 7, no. 4, p. 1–7.

Gurnis, M., Mitrovica, J.X., Ritsema, J., and van Heijst, H.-J., 2000, Constraining mantle density structure using geological evidence of surface uplift rates: The case of the African superplume: Geochemistry, Geophysics, Geosystems, v. 1, no. 1999GC000035.

Hager, H.H., 1984, Subducted slabs and the geoid: Constraints on mantle rheology and flow: Journal of Geophysical Research, v. 89, p. 6003–6015.

Jordan, T.H., 1978, Composition and development of the continental tectosphere: Nature, v. 274, p. 544–548.

Karato, J., 1993, Importance of anelasticity in the interpretation of seismic tomography: Geophysical Research Letters, v. 20, p. 1623–1626.

Keen, C.E., 1985, The dynamics of rifting: Deformation of the lithosphere by active and passive driving mechanisms: Royal Astronomical Society Geophysical Journal, v. 80, p. 95–120.

Laske, G., Masters, G., and Reif, C., 2002, CRUST 2.0: A new global crustal model at 2 × 2 degrees: http://mahi.ucsd.edu/Gabi/rem.html.

Levin, V., and Park, J., 2000, Shear zones in the Proterozoic lithosphere of the Arabian Shield and the nature of the Hales discontinuity: Tectonophysics, v. 323, p. 131–148.

Lithgow-Bertelloni, C., and Silver, P.G., 1998, Dynamic topography, plate driving forces and the African superswell: Nature, v. 395, p. 269–272.

Ni, S., Tan, E., and Helmberger, D., 2002, Sharp sides to the African superplume: Science, v. 296, p. 1850–1852.

Ritsema, J., and van Heijst, H.J., 2000, New seismic model of the upper mantle beneath Africa: Geology, v. 28, p. 63–66.

Ritsema, J., van Heijst, H.J., and Woodhouse, J.H., 1999, Complex shear wave velocity structure imaged beneath Africa and Iceland: Science, v. 286, p. 1925–1928.

Royden, L., and Keen, C.E., 1980, Rifting process and thermal evolution of the continental margin of eastern Canada determined from subsidence curves: Earth and Planetary Science Letters, v. 51, p. 343–361.

Solheim, L.P., and Peltier, W.R., 1994, Avalanche effects in phase transition modulated thermal convection: A model of Earth's mantle: Journal of Geophysical Research, v. 99, p. 6997–7018.

van der Beek, P., Cloetingh, S., and Andriessen, P., 1994, Mechanisms of extensional basin formation and vertical motions at rift flanks: Constraints from tectonic modeling and fission-track thermochronology: Earth and Planetary Science Letters, v. 121, p. 417–433.

Weissel, J.K., and Karner, G.D., 1989, Flexural uplift of rift flanks due to mechanical unloading of the lithosphere during extension: Journal of Geophysical Research, v. 94, p. 13,919–13,949.

Wernicke, B., 1985, Uniform-sense normal simple shear of the continental lithosphere: Canadian Journal of Earth Sciences, v. 22, p. 108–125.

White, R.S., and McKenzie, D.P., 1989, Magmatism at rift zones: The generation of volcanic continental margins and flood basalts: Journal of Geophysical Research, v. 94, p. 7685–7729.

Wolfe, C.J., Vernon, F.L., III, and Al-Amri, A., 1999, Shear-wave splitting across western Saudi Arabia: The pattern of upper mantle anisotropy at a Proterozoic shield: Geophysical Research Letters, v. 26, p. 779–782.

Manuscript received 17 March 2003
Revised manuscript received 18 June 2003
Manuscript accepted 8 July 2003

Printed in USA